Journal of Computational Mathematics
Vol.30, No.5, 2012, 504–516.

http://www.global-sci.org/jcm
doi:10.4208/jcm.1203-m3725

A NUMERICAL METHOD FOR SOLVING THE ELLIPTIC INTERFACE PROBLEMS WITH MULTI-DOMAINS AND TRIPLE JUNCTION POINTS*

Songming Hou Liqun Wang Wei Wang
Department of Mathematics and Statistics, Louisiana Tech University, Ruston, LA 71272, USA
Email: shou@latech.edu wliqunhmily@gmail.com htprww@gmail.com

Abstract

Elliptic interface problems with multi-domains and triple junction points have wide applications in engineering and science. However, the corner singularity makes it a challenging problem for most existing methods. An accurate and efficient method is desired. In this paper, an efficient non-traditional finite element method with non-body-fitting grids is proposed to solve the elliptic interface problems with multi-domains and triple junctions. The resulting linear system of equations is positive definite if the matrix coefficients for the elliptic equations in the domains are positive definite. Numerical experiments show that this method is about second order accurate in the L^∞ norm for piecewise smooth solutions. Corner singularity can be handled in a way such that the accuracy does not degenerate. The triple junction is carefully resolved and it does not need to be placed on the grid, giving our method the potential to treat moving interface problems without regenerating mesh.

Mathematics subject classification: 65N06, 65B99.
Key words: Elliptic equations, Non-body-fitting mesh, Finite element method, Triple junction, Jump condition.

1. Introduction

Elliptic interface problems have wide applications in a variety of disciplines. However, designing highly efficient methods for these problems is a difficult job, especially with multi-domains and triple junctions. In the past three decades, much attention has been paid to the numerical solution of elliptic equations with discontinuous coefficients and singular sources on regular Cartesian grids since the pioneering work of Peskin [22] on the first order accurate immersed boundary method. In many applications, particularly for free boundary and moving interface problems, simple Cartesian grids are preferred. In this way, the procedure of generating an unstructured grid can be bypassed, and well developed fast solvers on Cartesian grids can be utilized. With a fixed unstructured grid for moving interface problem, one cannot ensure the triple junction point is a grid point. Without careful treatment, the accuracy is compromised when the triple junction point is not a grid point.

Motivated by the immersed boundary method, to improve accuracy, in [10], the "immersed interface" method (IIM) was presented. This method achieves second order accuracy by incorporating the interface conditions into the finite difference stencil in a way that preserves the interface conditions in both solution and its flux, $[u] \neq 0$ and $[\beta u_n] \neq 0$. The corresponding linear system is sparse, but may not be symmetric or positive definite if there is a jump in the

* Received May 5, 2011 / Revised version received February 1, 2012 / Accepted March 18, 2012 /
Published online September 24, 2012 /

coefficient. Various applications and extensions of IIM are discussed in [4, 14]. In [11], a fast iterative method using the augmented IIM was developed for Poisson equations with piecewise constant but discontinuous coefficient. The number of calls to the fast Poisson solver of the method is independent of the jump in the coefficient and the mesh size.

In [12, 13], the immersed finite element methods (IFEM) are developed using non-body-fitted Cartesian meshes for homogeneous jump conditions. The idea is to modify the basis functions so that the homogeneous jump conditions are satisfied. Both non-conforming and conforming IFEM are developed in [13] for 2D problems. Numerical evidence shows that IFEM of the conforming version achieves second order accuracy in the L^∞ norm, and higher than first order for its non-conforming version. In [24], the IFEM is further developed to deal with non-homogeneous jump conditions. The non-conforming immersed finite element methods are also developed for elasticity equations in [5, 24].

In [11], a fast iterative method in conjunction with the "immersed interface" method has been developed for constant coefficient problems with the interface conditions $[u] = 0$ and $[\beta u_n] \neq 0$. Numerical results show that this method's conforming version achieves second order accuracy in the L^∞ norm, and higher than first order for its non-conforming version.

In [7], a non-traditional finite element formulation for solving elliptic equations with smooth or sharp-edged interfaces was proposed with non-body-fitting grids for $[u] \neq 0$ and $[\beta u_n] \neq 0$. It achieved second order accuracy in the L^∞ norm for smooth interfaces and about 0.8th order for sharp-edged interfaces. In [8], the method is modified and improved to close to 2nd order accurate for sharp-edged interfaces, and it is extended to handle general elliptic equations with matrix coefficient and lower order terms. The resulting linear system is non-symmetric but positive definite. In [9], the work was generalized to solve the elasticity interface problems. In [26], the matched interface and boundary (MIB) method was proposed to solve elliptic equations with smooth interfaces. In [25], the MIB method was generalized to treat sharp-edged interfaces. With an elegant treatment, second order accuracy was achieved in the L^∞ norm. Also, there has been a large body of work from the finite volume perspective for developing high order methods for elliptic equations in complex domains, such as [1], [19] for two dimensional problems and [20] for three dimensional problems. Another class of methods is the Boundary Condition Capturing Method [16–18].

Although there are many different methods above in the literature for solving the elliptic interface problems with two domains, the elliptic interface problems with multi-domains and triple junctions have not been extensively studied. The new challenges include the treatment of the triple junction point and the added complexity of the problem. In [23], the MIB method is generalized to solve the elliptic interface problems with multi-domains. Numerical evidence shows second order accuracy.

Based on the method in [8], in this paper we propose a numerical method for solving the elliptic problem in multi-domains. We propose an accurate treatment for the triple junction point shown in Figure 3.1. The resulting linear system is positive definite if the matrix coefficients $\beta_i,\ i = 1, 2, 3$ for the elliptic equation in three domains are positive definite. This method is not just a trivial extension of the one in [8], as the triple junction point has to be carefully studied. Numerical results demonstrate about second order accuracy for the method, even with presence of corner singularity. Compared with the existing method [23] for the same setup of the problem, there are two advantages of our method: one is the positive definiteness of the coefficient matrix, the other is the generalization to matrix coefficients β_i instead of scalar coefficients in [23].

2. Equations and Weak Formulation

Consider an open bounded domain $\Omega \subset R^d$. Let Γ be an interface of co-dimension $d-1$, which divides Ω into disjoint open subdomains, Ω_1, Ω_2 and Ω_3, hence $\Omega = \Omega_1 \bigcup \Omega_2 \bigcup \Omega_3 \bigcup \Gamma$, see Figure 2.1. Assume that the boundary $\partial\Omega$ and the boundary of each subdomain $\partial\Omega_{1,2,3}$ are Lipschitz continuous as submanifolds. Since $\partial\Omega_{1,2,3}$ are Lipschitz continuous, so is Γ. A unit normal vector of Γ can be defined a.e. on Γ, see Section 1.5 in [6].

Note that although for simplicity of discussion the above setup is for three domains with a triple junction, the method proposed in this paper works for multi-domains with many triple junction points since the treatments are local.

We seek solutions of the variable coefficient elliptic equation away from the interface Γ given by

$$-\bigtriangledown \cdot(\beta(x) \bigtriangledown u(x)) = f(x), \quad x \in \Omega \setminus \Gamma \tag{2.1}$$

in which $x = (x_1, ..., x_d)$ denotes the spatial variables and $\bigtriangledown$ is the gradient operator. The coefficient $\beta(x)$ is assumed to be a $d \times d$ matrix that is uniformly elliptic on each disjoint subdomain, Ω_1, Ω_2 and Ω_3, and its components are continuously differentiable on each disjoint subdomain, but they may be discontinuous across the interface Γ. The right-hand side $f(x)$ is assumed to lie in $L^2(\Omega)$.

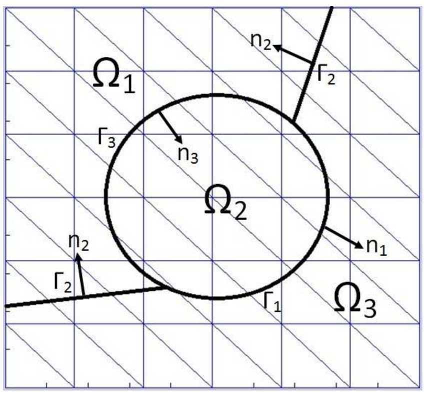

Fig. 2.1. A uniform triangulation.

Consider the problem on the rectangular domain $\Omega = (x_{min}, x_{max}) \times (y_{min}, y_{max}) = \Omega_1 \bigcup \Omega_2 \bigcup \Omega_3$. $\Gamma_j,\ j = 1, 2, 3$

$$\begin{cases} -\nabla \cdot (\beta_1 \nabla u_1) = f_1, \ \texttt{in}\ \Omega_1, \\ -\nabla \cdot (\beta_2 \nabla u_2) = f_2, \ \texttt{in}\ \Omega_2, \\ -\nabla \cdot (\beta_3 \nabla u_3) = f_3, \ \texttt{in}\ \Omega_3. \end{cases} \tag{2.2}$$

Given functions a and b along the interface $\Gamma = \Gamma_1 \bigcup \Gamma_2 \bigcup \Gamma_3$, we prescribe the jump conditions

$$\begin{cases} [u]_{\Gamma_1} := u_2 - u_3 = a_1, \ \texttt{on}\ \Gamma_1, \\ [u]_{\Gamma_2} := u_3 - u_1 = a_2, \ \texttt{on}\ \Gamma_2, \\ [u]_{\Gamma_3} := u_1 - u_2 = a_3, \ \texttt{on}\ \Gamma_3, \\ [\beta \nabla u]_{\Gamma_1} := (\beta_2 \nabla u_2 - \beta_3 \nabla u_3) \cdot n_1 = b_1, \ \texttt{on}\ \Gamma_1, \\ [\beta \nabla u]_{\Gamma_2} := (\beta_3 \nabla u_3 - \beta_1 \nabla u_1) \cdot n_2 = b_2, \ \texttt{on}\ \Gamma_2, \\ [\beta \nabla u]_{\Gamma_3} := (\beta_1 \nabla u_1 - \beta_2 \nabla u_2) \cdot n_3 = b_3, \ \texttt{on}\ \Gamma_3. \end{cases} \tag{2.3}$$

The "1,2,3" subscripts refer to limits taken from within the subdomains $\Omega_{1,2,3}$.

Finally, we prescribe boundary conditions

$$\begin{cases} u_1 = g_1, \ \texttt{on}\ \partial\Omega \bigcap \partial\Omega_1, \\ u_2 = g_2, \ \texttt{on}\ \partial\Omega \bigcap \partial\Omega_2, \\ u_3 = g_3, \ \texttt{on}\ \partial\Omega \bigcap \partial\Omega_3. \end{cases} \tag{2.4}$$

The interfaces prescribed by the zero level-set $\{(x,y) \in \Omega_j \mid \phi_j(x,y) = 0\}$ of a level-set function $\phi_j(x,y)$, which have the following properties:

$$\phi_1(x,y) \begin{cases} < 0, \ (x,y) \in \Omega_3, \\ = 0, \ (x,y) \in \Gamma_1, \\ > 0, \ (x,y) \in \Omega_2, \end{cases}$$

$$\phi_2(x,y) \begin{cases} < 0, \ (x,y) \in \Omega_1, \\ = 0, \ (x,y) \in \Gamma_2, \\ > 0, \ (x,y) \in \Omega_3, \end{cases}$$

$$\phi_3(x,y) \begin{cases} < 0, \ (x,y) \in \Omega_2, \\ = 0, \ (x,y) \in \Gamma_3, \\ > 0, \ (x,y) \in \Omega_1. \end{cases}$$

The unit normal vector of Γ_j is $n_j = \frac{\nabla \phi_j}{|\nabla \phi_j|}$ pointing from $\Omega_j^- := \{(x,y) \in \Omega \mid \phi_j(x,y) \le 0\}$ to $\Omega_j^+ = \{(x,y) \in \Omega \mid \phi_j(x,y) \ge 0\}$ for $j = 1, 2, 3$.

We use the weak formulation in [8] for the elliptic equation with matrix coefficient and define the inner product:

$$B\left[u,v\right] = \int_{\Omega_1} \beta \bigtriangledown u \cdot \bigtriangledown v + \int_{\Omega_2} \beta \bigtriangledown u \cdot \bigtriangledown v + \int_{\Omega_3} \beta \bigtriangledown u \cdot \bigtriangledown v. \tag{2.5}$$

Definition 2.1. *A function u (the space of u is defined in [8])is a weak solution of equation* 2.1-2.4*, if u satisfies, for all $\psi \in H_0^1(\Omega)$,*

$$\int_{\Omega_1} \beta \bigtriangledown u \cdot \bigtriangledown \psi + \int_{\Omega_2} \beta \bigtriangledown u \cdot \bigtriangledown \psi + \int_{\Omega_3} \beta \bigtriangledown u \cdot \bigtriangledown \psi = \int_{\Omega} f\psi + \int_{\Gamma} b\psi. \tag{2.6}$$

A classical solution of equation 2.1-2.4, $u|_{\Omega_{1,2,3}} \in C^2(\overline{\Omega_{1,2,3}})$ is necessarily a weak solution. Because all the subdomains' boundaries $\partial\Omega_{1,2,3}$ are Lipschitz continuous, the integration by parts are legal in each subdomain, $\Omega_{1,2,3}$.

It is shown in [6] that corner singularity could develop at the triple junction point with $f = 0$ in all the three domains. In this case, the solutions are in C^1 but not in C^2. Special numerical treatment is necessary to avoid a degeneracy in the convergence order, which will be discussed in Section 3. A numerical example for such case is provided in Section 4.

We have the following theorem:

Theorem 2.1. *If $f \in L^2(\Omega)$, and a, b $\in H^1(\Omega)$, then there exists a unique weak solution of equation* 2.2-2.4.

Proof. See Theorem 2.1 in [7].

3. Numerical Method

In this paper, we restrict ourselves to a rectangular domain $\Omega = (x_{min}, x_{max}) \times (y_{min}, y_{max})$ in the plane, and β is a 2×2 matrix that is uniformly elliptic in each subdomain. Given positive integers I and J, set $\Delta x = (x_{max} - x_{min})/I$ and $\Delta y = (y_{max} - y_{min})/J$. We define a uniform Cartesian grid $(x_i, y_j) = (x_{min} + i\Delta x, y_{min} + j\Delta y)$ for $i = 0, ..., I$ and $j = 0, ..., J$. Each (x_i, y_j) is called a grid point. For the case $i = 0, I$ or $j = 0, J$, a grid point is called a boundary point, otherwise it is called an interior point. The grid size is defined as $h = max(\Delta x, \Delta y) > 0$.

Two sets of grid functions are needed and they are denoted by

$$H^{1,h}_{\pm} \quad = \quad \{\omega^h = (\omega_{i,j}) : 0 \le i \le I, 0 \le j \le J\},$$

and

$$H^{1,h}_{0,\pm} \quad = \quad \{\omega^h = (\omega_{i,j}) \in H^{1,h}_{\pm} : \omega_{i,j} = 0 \texttt{ if } i = 0, I \texttt{ or } j = 0, J\}.$$

We cut every rectangular region $[x_i, x_{i+1}] \times [y_j, y_{j+1}]$ into two pieces of right triangular regions: one is bounded by $x = x_i, y = y_j$ and $y = \frac{y_{j+1}-y_j}{x_i - x_{i+1}}(x - x_{i+1}) + y_j$, and the other is bounded by $x = x_{i+1}, y = y_{j+1}$ and $y = \frac{y_{j+1}-y_j}{x_i - x_{i+1}}(x - x_{i+1}) + y_j$. Collecting all those triangular regions, we obtain a uniform triangulation $T^h : \bigcup_{K\in T^h} K$, see Fig.2.1. We can also choose the hypotenuse to be $y = \frac{y_{j+1}-y_j}{x_{i+1}-x_i}(x - x_i) + y_j$, and get another uniform triangulation from the same Cartesian grid. There is no conceptual difference for our method on these two triangulations.

A cell K belongs to one of the three sets below:

$$\Lambda_1 = \{\triangle_k \subset \Omega : k_1, k_2, k_3 \texttt{ are in the same domain among } \Omega_j,\ j = 1, 2, 3\},$$
$$\Lambda_2 = \{\triangle_k \subset \Omega : k_1, k_2, k_3 \texttt{ are in two different domains among } \Omega_j,\ j = 1, 2, 3\},$$
$$\Lambda_3 = \{\triangle_k \subset \Omega : k_1, k_2, k_3 \texttt{ are in three different domains of } \Omega_j,\ j = 1, 2, 3\}.$$

If $K \in \Lambda_1$, it is a normal finite element. If $K \in \Lambda_2$, it has the same definition in **Section 3**, [8]. If $K \in \Lambda_3$, Fig 3.1 show the interfaces inside K.

Theorem 3.1. *For all $u^h \in H^{1,h}_{\pm}, U^h(u^h)$ can be constructed uniquely, provided T^h, ϕ, a and b are given.*

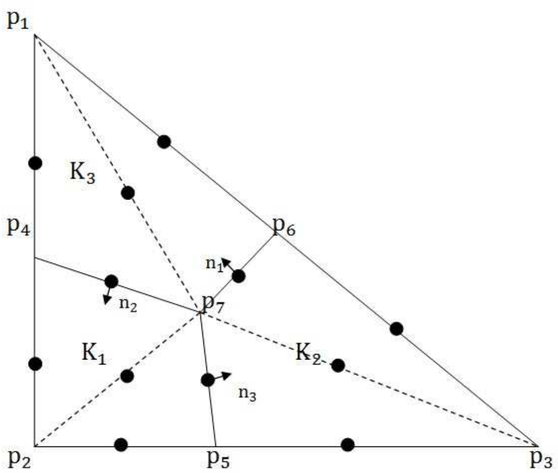

Fig. 3.1. One Triangle Cell.

Proof. see Theorem 3.1 in [8].

Lemma 3.1. *The coefficient matrix A generated by the method above is independent of $a_j(x,y)$ and $b_j(x,y)$, $j=1,2,3$.*

Proof. See Lemma 3.2 in [8].

Theorem 3.2. *The coefficient matrix $A=(a_{ij})_{n\times n}$ generated by the method above is positive definite if β_j, $j=1,2,3$ are continuous and positive definite.*

Proof. We want to show that for any vector $c\in R^n$, $c^TAc>0$. Since

$$c^TAc=\sum_{i,j=1}^{n}a_{ij}c_ic_j=B\left[\sum_{i=1}^{n}c_iu^i,\sum_{i=1}^{n}c_i\psi^i\right]$$

where u^i are basis functions for the solution and ψ^i are the test functions. For i-th grid point, u^i and ψ^i both have non-zero support only on the six triangles which have a vertex on the i-th grid point. So we can decompose u^i into $u^i=\sum_{j=1}^{6}u^i_j$, where each u^i_j has non-zero support only on the j-th triangle around the i-th grid point.

Let m be the number of triangles on the whole domain $\Omega=\bigcup_{k=1}^{m}\triangle_k$. We can rewrite the summation of u^i over all the triangles:

$$\sum_{i=1}^{n}c_iu^i=\sum_{i=1}^{n}\sum_{j=1}^{6}c_iu^i_j=\sum_{k=1}^{m}U_k,$$

where U_k is defined on $\triangle_k=\triangle_{k_1k_2k_3}$, and $U_k=c_{k_1}u_{k_1}+c_{k_2}u_{k_2}+c_{k_3}u_{k_3}$, k_1,k_2,k_3 are the three vertices of $\triangle_k$.

Similarly, we can rewrite the summation of ψ^i over all the triangles:

$$\sum_{i=1}^{n}c_i\psi^i=\sum_{i=1}^{n}\sum_{j=1}^{6}c_i\psi^i_j=\sum_{k=1}^{m}\Psi_k,$$

with $\Psi_k=c_{k_1}\psi_{k_1}+c_{k_2}\psi_{k_2}+c_{k_3}\psi_{k_3}$.

Consider sets

$$\Lambda_1=\{\triangle_k\subset\Omega:k_1,k_2,k_3\ \texttt{are in the same domain among}\ \Omega_j,\ j=1,2,3\},$$
$$\Lambda_2=\{\triangle_k\subset\Omega:k_1,k_2,k_3\ \texttt{are in two different domains among}\ \Omega_j,\ j=1,2,3\},$$
$$\Lambda_3=\{\triangle_k\subset\Omega:k_1,k_2,k_3\ \texttt{are in three different domains of}\ \Omega_j,\ j=1,2,3\}.$$

Then

$$\sum_{k=1}^{m}U_k=\sum_{\triangle_k\in\Lambda_1}U_k+\sum_{\triangle_k\in\Lambda_2}U_k+\sum_{\triangle_k\in\Lambda_3}U_k,$$
$$\sum_{k=1}^{m}\Psi_k=\sum_{\triangle_k\in\Lambda_1}\Psi_k+\sum_{\triangle_k\in\Lambda_2}\Psi_k+\sum_{\triangle_k\in\Lambda_3}\Psi_k.$$

The difference between U_k and Ψ_k is, U_k satisfies the jump conditions on the interface and Ψ_k is a simple linear function on $\triangle_k$. So when $\triangle_k\in\Lambda_1$, there is no jump in $\triangle_k$. Thus

$$U_k(x,y)=\Psi_k(x,y),\ (x,y)\in\triangle_k,\ \triangle_k\in\Lambda_1.$$

When $\triangle_k \in \Lambda_2$ or $\triangle_k \in \Lambda_3$, by adjusting jump conditions to $a_j(x,y)=0$ and $b_j(x,y)=0$ we can obtain that

$$U_k(x,y) = \Psi_k(x,y), \ \ (x,y) \in \triangle_k.$$

Note that Lemma 3.1 says the matrix A for the generated linear system is independent of the the jump conditions. Therefore the above choice of jump conditions would not change the matrix A.

We combine the results in $\Lambda_j, \ j=1,2,3$ to obtain

$$\sum_{i=1}^{n} c_i u^i = \sum_{i=1}^{n} c_i \psi^i.$$

It now follows from the positive definiteness of β that

$$c^T A c = B\left[\sum_{i=1}^{n} c_i u^i, \sum_{i=1}^{n} c_i \psi^i\right] > 0.$$

Therefore, A is positive definite. $\square$

Remark 3.1. A positive definite matrix has positive determinant, and is therefore invertible. It also has an LDM^T factorization where $D = diag(d_i)$ and $d_i > 0$, and L, M are lower triangular. The linear system $Ax = b$ can be solved efficiently. Although a rigorous proof requires the continuity of the coefficients, all our numerical examples show that even with jumps in the coefficients across the interface, the matrix A is (non-symmetric) positive definite.

Remark 3.2. The above results are valid with presence of corner singularity. However, without a special treatment, the convergence order would degenerate in this case. In order to obtain second order accuracy, one could use a procedure similar to the one discussed in [25] and [23]. This is demonstrated by a numerical example in Section 4.

4. Numerical Experiments

In all numerical experiments below, the level-set function $\phi_j(x,y)$, the coefficients $\beta_j(x,y)$, and the solutions u_j are given for $j=1,2,3$. Hence f_j, a_j, b_j can be calculated on the whole domain Ω. g_j is obtained as a proper Dirichlet boundary condition, since the solutions are given.

All errors in solutions are measured in the L^∞ norm in the whole domain Ω.

We present three numerical examples to demonstrate the effectiveness of our method.

Example 1. Our first example has two triple junction points of intersection of three domains. The level-set function $\phi_j(x,y)$, the coefficients $\beta_j(x,y)$, and the solution $u_j(x,y)$ for $j=1,2,3$

Table 4.1: Numerical results for three-domain problem with two triple junction points

$n_x \times n_y$	Err in U	Order
40×40	5.4492e-002	
80×80	1.6279e-002	1.74
160×160	4.3505e-003	1.90
320×320	1.0927e-003	1.99

are given as follows:

$$
\begin{aligned}
\phi_1(x,y) &= -((x+0.17)^2+y^2-0.317^2),\\
\phi_2(x,y) &= (x-0.153)^2+y^2-0.41^2,\\
\phi_3(x,y) &= (x+0.17)^2+y^2-0.317^2,\\
\beta_1^+(x,y) &= \begin{pmatrix} x^2+y^2+1 & x^2+y^2+2 \\ x^2+y^2+2 & x^2+y^2+5 \end{pmatrix},\\
\beta_2^+(x,y) &= \begin{pmatrix} x^4+y^4+1 & x^4+y^4+2 \\ x^4+y^4+2 & x^4+y^4+5 \end{pmatrix},\\
\beta_3^+(x,y) &= \begin{pmatrix} x^2+y^4+1 & x^2+y^4+2 \\ x^2+y^4+2 & x^2+y^4+5 \end{pmatrix},\\
u_1(x,y) &= x+e^y+1,\\
u_2(x,y) &= \sin(2\pi x)\sin(2\pi y)+6,\\
u_3(x,y) &= x^2+y^3+\sin(x+y).
\end{aligned}
$$

Fig. 4.1 shows the numerical solution with our method using a 40×40 grid. Table 4.1 shows the error on different grids. The numerical result shows close to second order accuracy in the L^∞ norm for the solution.

Example 2. Our second example is two circles circumscribed with each other. The level-set function $\phi_j(x,y)$, the coefficients $\beta_j(x,y)$, and the solution $u_j(x,y)$ for $j=1,2,3$ are given as

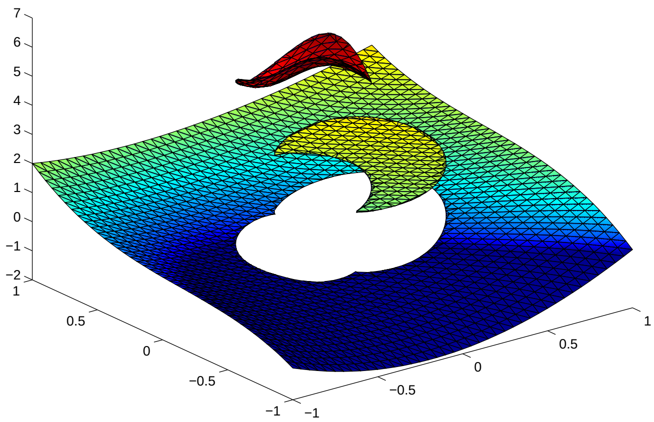

Fig. 4.1. Three domain problem with two triple junction points.

Table 4.2: Numerical results for two circles circumscribed.

$n_x \times n_y$	Err in U	Order
40×40	9.5274e-003	
80×80	2.6414e-003	1.85
160×160	7.7858e-004	1.76
320×320	2.1667e-004	1.84

follows:

$$
\begin{aligned}
\phi_1(x,y) &= -((x+0.35)^2+y^2-0.35^2),\\
\phi_2(x,y) &= (x-0.35)^2+y^2-0.35^2,\\
\phi_3(x,y) &= x,\\
\beta_1^+(x,y) &= \begin{pmatrix} x^2+y^2+1 & x^2+y^2+2 \\ x^2+y^2+2 & x^2+y^2+5 \end{pmatrix},\\
\beta_2^+(x,y) &= \begin{pmatrix} x^4+y^4+1 & x^4+y^4+2 \\ x^4+y^4+2 & x^4+y^4+5 \end{pmatrix},\\
\beta_3^+(x,y) &= \begin{pmatrix} x^2+y^4+1 & x^2+y^4+2 \\ x^2+y^4+2 & x^2+y^4+5 \end{pmatrix},\\
u_1(x,y) &= 5x+6y+1,\\
u_2(x,y) &= -5x+6y+1,\\
u_3(x,y) &= 2y^2+\sin(2\pi x)-2.
\end{aligned}
$$

Fig. 4.2 shows the numerical solution with our method using a 40×40 grid. Table 4.2 shows the error on different grids. The numerical result shows close to second order accuracy in the L^∞ norm for the solution.

Example 3. Our third example is a circle circumscribed on a star. The level-set function $\phi_j(x,y)$, the coefficients $\beta_j(x,y)$, and the solution $u_j(x,y)$ for $j=1,2,3$ are given as follows:

$$
\begin{aligned}
\phi_1(r,\theta) &= -(\frac{R\sin(\theta_t/2)}{\sin(\theta_t/2+\theta-\theta_r-2\pi(i-1)/5)}-r\\
&\qquad \theta_r+\pi(2i-2)/5\le\theta<\theta_r+\pi(2i-1)/5),\\
\phi_1(r,\theta) &= -(\frac{R\sin(\theta_t/2)}{\sin(\theta_t/2-\theta+\theta_r-2\pi(i-1)/5)}-r\\
&\qquad \theta_r+\pi(2i-3)/5\le\theta<\theta_r+\pi(2i-2)/5),
\end{aligned}
$$

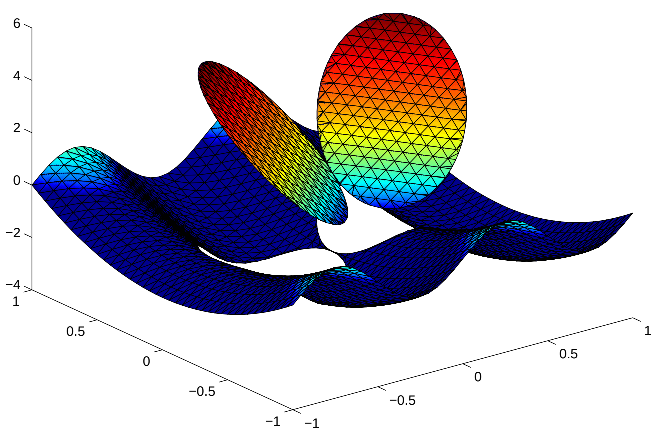

Fig. 4.2. Two circles circumscribed.

Table 4.3: Numerical results for the Star in Circle example.

$n_x \times n_y$	Err in U	Order
40×40	1.7135e-002	
80×80	5.2382e-003	1.71
160×160	1.3995e-003	1.90
320×320	3.5629e-004	1.97

with $\theta_t = \pi/5,\ \theta_r = \pi/7,\ R = 6/7$ and $i = 1, 2, 3, 4, 5$.

$$
\begin{aligned}
&\phi_2(x,y) = x^2 + y^2 - (6/7)^2,\\
&\phi_3(x,y) = -(x^2 + y^2 - (6/7)^2),\\
&\beta_1^+(x,y) = \begin{pmatrix} x^2+y^2+1 & x^2+y^2+2 \\ x^2+y^2+2 & x^2+y^2+5 \end{pmatrix},\\
&\beta_2^+(x,y) = \begin{pmatrix} x^2-y^2+3 & x^2-y^2+1 \\ x^2-y^2+1 & x^2-y^2+4 \end{pmatrix},\\
&\beta_3^+(x,y) = \begin{pmatrix} xy+2 & xy+1 \\ xy+1 & xy+3 \end{pmatrix},\\
&u_1(x,y) = 2y + 1 + 0.1\sin(2\pi(x^2+y)),\\
&u_2(x,y) = 0,\\
&u_3(x,y) = y^3 + e^x + 1.
\end{aligned}
$$

Fig. 4.3 shows the numerical solution with our method using a 40×40 grid. Table 4.3 shows the error on different grids. The numerical result shows close to second order accuracy in the L^∞ norm for the solution.

Example 4. Our final example has a triple-junction point at which corner singularity of solution is present for three domains. The level-set function $\phi_j(x,y)$, the coefficients $\beta_j(x,y)$,

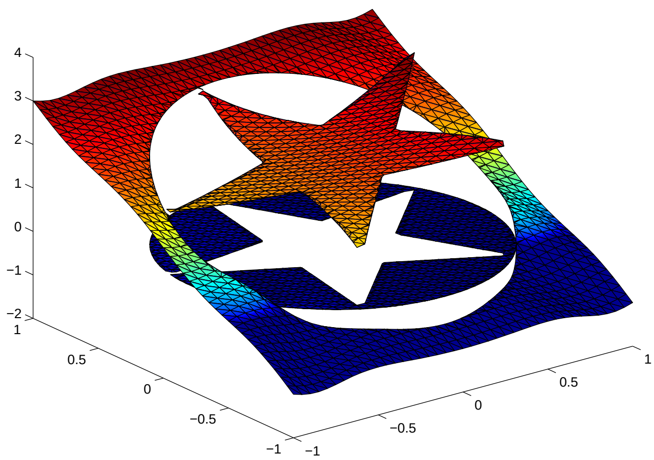

Fig. 4.3. Star in circle.

Table 4.4: Numerical results for triple junction with corner singularity.

$n_x \times n_y$	Err in U	Order
40×40	1.2742e-002	
80×80	3.5392e-003	1.85
160×160	8.8849e-004	1.99
320×320	2.1758e-004	2.03

and the solution $u_j(x,y)$ for $j=1,2,3$ are given as follows:

$$\begin{aligned}
&\phi_1(x,y)=x+0.1y, &&\beta_1^+(x,y)=\begin{pmatrix}1&0\\0&1\end{pmatrix},\\
&\phi_2(x,y)=-x-0.2y, &&\beta_2^+(x,y)=\begin{pmatrix}2&0\\0&2\end{pmatrix},\\
&\phi_3(x,y)=y+0.03x, &&\beta_3^+(x,y)=\begin{pmatrix}3&0\\0&3\end{pmatrix},\\
&u_1(x,y)=x+e^y+1+w_1(x,y),\\
&u_2(x,y)=\sin(x)+6+w_2(x,y),\\
&u_3(x,y)=x^2+y^3+\sin(x+y)+w_3(x,y),
\end{aligned}$$

where w_1, w_2, w_3 are the singularity terms:

$$w_i(r,\theta)=r^{\frac{\pi}{\alpha_i}}\sin\left(\frac{\pi}{\alpha_i}(\theta-\theta_i)\right),$$

with $\alpha_1=1.798,\quad \theta_1=-0.030,\quad \alpha_2=1.441,\quad \theta_2=-1.471,\quad \alpha_3=3.049,\quad \theta_3=1.768$, The singular terms are derived from the Laplace equation in polar coordinates, see [6] for details.

By a procedure similar to the one implemented in [25] and [23], we multiply the solution by a polynomial $(x^2+y^2)^2$. Corner singularity can be removed so that the accuracy does not degenerate.

Fig. 4.4 shows the numerical solution after multiplied with $(x^2+y^2)^2$ using a 40×40 grid.

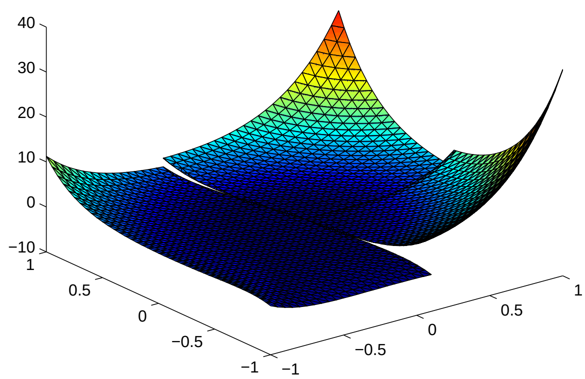

Fig. 4.4. Dealing with corner singularity.

Table 4.4 shows the error on different grids. The numerical result shows close to second order accuracy in the L^∞ norm for the solution.

5. Conclusion

In this paper, we modified the method in [8] to solve the elliptic interface problem in multi-domains with triple junctions. The matrix for the linear system generated by our method is positive definite (but not symmetric) if the matrix coefficients for the elliptic equation in three domains are positive definite. Through numerical experiments, our method is shown to be close to second order accuracy in the L^∞ norm, thanks to our careful treatment of the triple junction points. By using a standard procedure of multiplying by a polynomial, the accuracy does not degenerate with the presence of corner singularities.

Acknowledgments. This research is partially supported by Louisiana Board of Regents RCS Grant No. LEQSF(2008-11)-RD-A-18.

References

[1] P. Colella and H. Johansen, A Cartesian grid embedded boundary method for Poisson's equation on irregular domains. *J. Comput. Phys.*, **60** (1998), 85–147.

[2] M. Cisternino and L. Weynans, A parallel second order Cartesian method for elliptic interface problems, *Commun. Comput. Phys.*, **12** (2012), 1562–1587.

[3] M.-C. Lai, Y.-H. Tseng and H. Huang, Numerical simulation of moving contact lines with surfactant by immersed boundary method, *Commun. Comput. Phys.*, **8** (2010), 735–757.

[4] S. Deng, K. Ito and Z. Li, Three dimensional elliptic solvers for interface problems and applications, *J. Comput. Phys.*, **184** (2003), 215–243.

[5] Y. Gong and Z. Li, Immersed Interface Finite Element Methods for Elasticity Interface Problems with Non-homogeneous Jump Conditions, *Numerical Mathematics: Theory, Methods and Applications*, **3** (2010), 23-39.

[6] P. Grisvard, Elliptic problems in nonsmooth domains - monographs and studies in mathematics, *Pitman Advanced Publishing Program*, (1985), 0743–0329.

[7] S.-M. Hou and X.-D. Liu, A numerical method for solving variable coefficient elliptic equations with interfaces, *J. Comput. Phys.*, **202** (2005), 411–445.

[8] S.-M. Hou, W. Wang and L.-Q. Wang, Numerical method for solving matrix coefficient elliptic equation with sharp-edged interfaces, *J. Comput. Phys.*, **229** (2010), 7162–7179.

[9] S.-M. Hou and Z. Li, L.-Q. Wang and W. Wang, A numerical method for solving elasticity equations with interfaces, *Communication in Computational Physics*, **12**:2 (2012), 595-612.

[10] R.J. LeVeque and Z. Li, The immersed interface method for elliptic equations with discontinuous coefficients and singular sources, *SIAM J. Numer. Anal.*, **31** (1994), 1019-1044

[11] Z. Li, A fast iterative algorithm for elliptic interface problems. *SIAM J. Numer. Anal.*, **35** (1998), 230–254.

[12] Z. Li, The immersed interface method using a finite element formulation, *Applied Numer. Math.*, **27** (1998), 253–267.

[13] Z. Li, T. Lin and X. Wu, New Cartesian grid methods for interface problem using finite element formulation, *Numer. Math.*, **96** (2003), 61–98.

[14] Z. Li and K. Ito, The Immersed Interface Method: Numerical Solutions of PDEs Involving Interfaces and Irregular Domains, *SIAM, Philadelphia*, (2006).

[15] Z. Li and P. Song, An adaptive mesh refinement strategy for immersed boundary/interface methods, *Commun. Comput. Phys.*, **12** (2012), 515–527.

[16] X.-D. Liu and R. P. Fedkiw, and M. Kang, A boundary condition capturing method for Poisson's equation on irregular domains, *J. Comput. Phys.*, **160**:1 (2000), 151–178.

[17] X.-D. Liu and T. Sideris, Convergence of the ghost fluid method for elliptic equations with interfaces, *Math. Comp.*, **72** (2003).

[18] P. Macklin and J. S. Lowengrub, A New Ghost Cell / Level Set Method for Moving Boundary Problems: Application to Tumor Growth. *Journal of Scientific Computing*, **35** (2008), 266–299.

[19] M. Oevermann and R. Klein, A Cartesian grid finite volume method for elliptic equations with variable coefficients and embedded interfaces. *J. Comput. Phys.*, **219** (2006), 749–769.

[20] M. Oevermann, C. Scharfenberg and R. Klein. A sharp interface finite volume method for elliptic equations on Cartesian grids, *J. Comput. Phys.*, **228** (2009), 5184–5206.

[21] Z. Tan, D. V. Le, K. M. Lim and B. C. Khoo, An immersed interface method for the simulation of inextensible interfaces in viscous fluids, *Commun. Comput. Phys*, **11** (2012), 925–950.

[22] C. Peskin, Numerical analysis of blood flow in the heart, *J. Comput. Phys.*, **25** (1977), 220–252.

[23] K. Xia, M. Zhan and G.W. Wei, The matched interface and boundary (MIB) method for multi-domain elliptic interface problems, *J. Comput. Phys.*, **230** (2011) 8231–8258.

[24] X. Yang, B. Li and Z. Li, The immersed interface method for elasticity problems with interface, *Dynamics of Continuous, Discrete and Impulsive Systems*, **10** (2003), 783–808.

[25] S. Yu, Y. Zhou and G.W. Wei, Matched interface and boundary (MIB) method for elliptic problems with sharp-edged interfaces, *J. Comput. Phys.*, **224** (2007), 729–756.

[26] Y.C. Zhou, S. Zhao, M. Feig and G.W. Wei, High order matched interface and boundary method for elliptic equations with discontinuous coefficients and singular sources, *J. Comput. Phys.*, **213** (2006), 1–30.